Journal of Microencapsulation, 2011; 28(5): 455–463

ISSN 0265-2048 print/ISSN 1464-5246 online
DOI: 10.3109/02652048.2011.576787

informa
healthcare

Bioadhesive properties of poly(anhydride) nanoparticles coated with different molecular weights chitosan

Juan Manuel Llabot[1], Hesham Salman[2], Gioconda Millotti[3], Andreas Bernkop-Schnürch[3], Daniel Allemandi[1] and Juan Manuel Irache[2]

[1]*Departamento de Farmacia, Facultad de Ciencias Químicas, Universidad Nacional de Córdoba, Córdoba, Argentina,* [2]*Department of Pharmaceutics and Pharmaceutical Technology, University of Navarra, Spain, and* [3]*Department of Pharmaceutical Technology, Institute of Pharmacy, Leopold-Franzens-University Innsbruck, Innsbruck, Austria*

Abstract

The aim of this study was to develop and characterize the bioadhesive properties of poly(anhydride) nanoparticles coated with two types of low-molecular weight chitosan (CH20 of 20 kDa or CH50 of 50 kDa) or their thiolated conjugates. Nanoparticles were prepared by a solvent displacement method and characterized by measuring the size, zeta potential, morphology and composition. For bioadhesion studies, nanoparticles were fluorescently labelled with rhodamine B isothiocyanate. In all cases, coated nanoparticles showed a slightly higher size and lower negative zeta potential than uncoated nanoparticles. Nanoparticles coated with CH20 showed a higher adhesive capacity than uncoated nanoparticles. On the contrary, when nanoparticles were coated with CH50, the resulting carriers displayed a decreased ability to develop adhesive interactions within the gut. Finally, the coating of nanoparticles with thiolated chitosan improved their adhesive abilities. Poly(anhydride) nanoparticles coated with thiolated chitosan can be considered as promising bioadhesive particulate carriers for oral delivery strategies.

Keywords: Chitosan, thiolated chitosan, nanoparticles, bioadhesion, poly(anhydride)

Introduction

Nanoparticles have been proposed as drug carriers for the oral administration of poorly available molecules, protecting them from the degradation, such as peptides, proteins or DNA (Damge et al., 1988; Cui and Mumper, 2001; Soares et al., 2007; Perera et al., 2009). In addition, these colloidal carriers are able to modulate or control the release of the loaded compound in order to optimize its therapeutic level in the body compartments (Ambruosi et al., 2005; Huang et al., 2005; Esmaeili et al., 2008; Sahana et al., 2008). When administered by the oral route, polymeric nanoparticles constructed by bioadhesive polymers may develop adhesive interactions with components of the mucus layer or cells in the absorptive epithelium. This bioadhesion phenomenon may increase the residence time of nanoparticles in close contact with the mucosa (Ponchel and Irache, 1998), resulting in increased bioavailability of the loaded drug (Florence, 1997; Pandey et al., 2005).

It has been demonstrated that the surface properties of nanoparticles are a key factor influencing their *in vivo* fate (Damge et al., 1997). Thus, the coating of nanoparticles with hydrophilic polymers or macromolecules has become one of the main strategies to modify the biodistribution of nanoparticles in the body. In this context, the use of poly(ethyleneglycol) (PEG) or polysaccharides (i.e. dextran or chitosan) to coat polymeric nanoparticles or liposomes appears to provide an efficient steric physical barrier against non-specific protein adsorption, minimizing their capture by cells of the monocyte–macrophagic system

Address for correspondence: Juan Manuel Llabot, Departamento de Farmacia, Facultad de Ciencias Químicas, Universidad Nacional de Córdoba, Ciudad Universitaria, 5000 Córdoba, Argentina. Tel/Fax: +54 351 4334127. E-mail: jmllabot@fcq.unc.edu.ar
Juan M. Irache, Centro Galénico, Universidad de Navarra, Irunlarrea, 1; Ap. 177. 31080 Pamplona, Spain. Tel: +34 948425600. Fax: +34 948425649. E-mail: jmirache@unav.es

(Received 30 Nov 2010; accepted 28 Mar 2011)
http://www.informahealthcare.com/mnc

(Aumelas et al., 2007; Choi and Kim, 2007; Esmaeili et al., 2008).

Modification of the surface of nanoparticles with hydrophilic compounds (PEG or dextrans) can be an adequate strategy to obtain bioadhesive carriers for mucosal delivery and to target the small intestine (Yoncheva et al., 2005). Coating of nanoparticles with these hydrophilic macromolecules would facilitate their ''filtration'' through the mucus layer and their interaction directly with the surface of the enterocytes (Porfire et al., 2010).

Another interesting strategy to modulate the bioadhesive properties of polymeric nanoparticles would be their association with chitosan or its derivatives. Chitosan is a biodegradable, biocompatible and non-toxic polysaccharide, widely employed for pharmaceutical purposes (Thanou et al., 2001). Furthermore, it has been demonstrated that chitosan can strongly adhere to gastrointestinal mucus layers by the establishment of electrostatic interactions with sialic groups of mucin (Hassan and Gallo, 1990). In addition, chitosan can enhance the absorption of hydrophilic molecules by promoting a structural reorganization of the tight junction-associated proteins (Hassan and Gallo, 1990; Thanou et al., 2001; Van der Merwe et al., 2004). As chitosan derivatives, thiolated conjugates appear to offer a number of advantages for drug delivery purposes including comparatively high-bioadhesive, permeation-enhancing and cohesive properties.

Thus, the aim of this study was to develop and evaluate the bioadhesive properties of poly(methyl vinyl ether-co-maleic anhydride) nanoparticles when coated with low-molecular weight chitosan (20 and 50 kDa) or their thiolated conjugates (chitosan–thioglycolic acid conjugate, CH–TG).

Methods

Materials

Poly(methyl vinyl ether-co-maleic anhydride) or poly(anhydride) (Gantrez® AN 119) was kindly gifted by ISP (Barcelona, Spain). Chitosan (400 000 g/mol), thioglycolic acid and isopentane were purchased from Fluka (Buchs, Switzerland). Rhodamine B isothiocyanate (RBITC) and 3(dimethylaminopropyl)–N–ethylcarbodiimide hydrochloride (EDAC) was supplied by Sigma (Madrid, Spain). O.C.T.® was obtained from Sakura (Alphen aan den Rijn, The Netherlands). All other chemicals used were of reagent grade and obtained from Merck (Madrid, Spain).

Preparation of CH–TG

Depolymerization of chitosan

Chitosan was chemically treated with sodium nitrite in 6% (v/v) acetic acid to produce low-molecular mass chitosan following the method developed by Bravo-Osuna et al. (2007). Briefly, 100 mL of a 2% w/v commercial chitosan (400 000 g/mol) solution in acetic acid solution (6% v/v) was depolymerized at room temperature under stirring with 10 mL of $NaNO_2$ solutions in demineralized water at different concentrations (7.0% and 2.7%), in order to obtain the desired final molecular weight: 20 000, 50 000 g/mol, respectively. After 1 h of reaction, chitosan was precipitated by raising the pH to 9.0 with NaOH (4 M). The white-yellowish solid was filtered, extensively washed with acetone and redissolved in a minimum volume of acetic acid (0.1 M; around 20–30 mL). Purification was carried out two times by subsequent dialysis against demineralized water for 2 h and additionally overnight. The dialysed product was freeze-dried and the yellowish lyophilizate was then stored at 4°C. Products obtained were named as follows: CH20 (20 000 g/mol unmodified) and CH50 (50 000 g/mol unmodified) depending on its theoretical molecular weight.

Modification of chitosan with TGA

The inclusion of thiol groups in the hydrolysed (low molecular weight) was carried out following the method developed by Kast and Bernkop-Schnürch (2001). Briefly, 2 g of each unmodified polymer was dissolved in 16 mL HCl (1 M) and water to obtain a 1% (w/v) solution. Then, 2 g of thioglycolic acid was added to the chitosan solution. The pH was adjusted to 6 with 1 M NaOH. Afterwards, EDAC was added in final concentrations of either 50 mM (TGA) or 200 mM (TGB).

The pH was adjusted to 6 with 1 M NaOH and the reaction was allowed to proceed for 3 h under stirring. Afterwards, the polymers were dialysed against 5 L of water. The reaction mixture was then dialysed using membrane size: molecular weight cut-off 12 kDa, dialysis tubings, cellulose membrane (Sigma) for 3 days at 10°C in dark against 5 mM HCl, then two times against 5 mM HCl containing 1% (w/v) NaCl and finally against 1 mM HCl containing 1 mL of 1 M HCl, twice against 5 L of demineralized water containing 45 g NaCl and 1 mL of 5 N HCl and finally against 5 L of water containing 1 mL of 1 M HCl, the polymers were then freeze-dried.

Determination of the thiol group content

The degree of modification was determined *via* the Ellman's test. First, 0.5 mg of each sample was hydrated in 500 μL of Ellman's reagent (3 mg of 5,5-dithiobis(2-nitrobenzoic acid) (DTNB) dissolved in 10 mL of 0.5 M phosphate buffer (pH 8.0) was added. The samples were then incubated at room temperature for 2 h. Afterwards, 300 μL of each sample was measured in absorbancy at a wavelength of 450 nm with a microplate reader. Cysteine was used as a standard to measure a calibration curve.

The amount of disulphide bonds was determined as follows: First, 0.5 mg of the conjugate was hydrated in 1 mL of 50 mM phosphate buffer (pH 8.0) for 30 min. Afterwards, 600 μL of 3% sodium-borohydrate solution was added to the sample solutions and incubated for 2 h in an oscillating water bath at 37°C. Afterwards, 500 μL of 1 M HCl was added in order to stop the action of sodium-borohydrate. Consecutively, 1 mL of 1 M phosphate buffer (pH 8.5) and

Table 1. Main characteristics of the different synthesized chitosans used in this study.

Chitosan	Total thiols (μmol/g polymer)	Reduced thiols (μmol/g polymer)
CH20 (20.000 kDa)	–	–
CH20–TGA	82.93 ± 32.27	43.78 ± 3.59
CH20–TGB	403.76 ± 8.34	238.76 ± 19.01
CH50 (50.000 kDa)	–	–
CH50–TGA	90.58 ± 8.20	68.7 ± 2.67
CH50–TGB	496.31 ± 15.46	382.71 ± 27.75

Note: Data expressed as mean ± SD ($n = 3$).

200 μL of a 0.5% (w/v) DTNB dissolved in 0.5 M phosphate buffer pH 8.0 were added. After 30 min of incubation at room temperature, 200 μL was transferred to a 96-well plate and absorbance was measured as described above. The amount of disulphide bonds was calculated by subtracting the amount of free thiol groups from the total amount of thiol groups.

Preparation of poly(anhydride) nanoparticles

Poly(anhydride) nanoparticles were prepared by a modification of a solvent displacement method (Arbos et al., 2002). In brief, 100 mg of the copolymer between methyl vinyl ether and maleic anhydride (Gantrez AN®) was dissolved in 5 mL of acetone. Then, the nanoparticles were formed by the addition of 10 mL with 50:50 (v/v) ethanol/water. The organic solvents were eliminated under reduced pressure (Flawil, Büchi R-144, Switzerland). For chitosan coating, the freshly prepared nanoparticles were incubated with 0.5 mg of the different types of chitosan (Table 1) in the aqueous dispersion for 1 h at room temperature (chitosan/poly(anhydride) ratio: 0.5% w/w). Then, chitosan-coated nanoparticles were purified twice by centrifugation at 27 000 × g for 20 min (Sigma 3K30, Osterode am Harz, Germany). The supernatants resulting from the purification steps were recovered in order to quantify the unloaded chitosan by UV (Section 2.5), whereas the pellets were centrifuged again under the same conditions. Finally, nanoparticles were freeze-dried (Genesis 12EL, Virtis, New York, NY) after dispersion in 3 mL aqueous solution containing 5% sucrose as cryoprotector.

Uncoated (control nanoparticles, NP) were prepared in the same way in the absence of chitosan. For *in vivo* studies, the nanoparticles were fluorescently labelled by incubation with 1.25 mg of rhodamine B isothiocyanate (RBITC) for 5 min at room temperature.

Characterization of the nanoparticles

The particle size and the zeta potential of nanoparticles were determined by photon correlation spectroscopy (PCS) and electrophoretic laser Doppler anemometry, respectively, using a Zetamaster analyser system, at 25°C (Malvern Instruments, Malvern, UK). The diameter of the nanoparticles was determined after dispersion in ultrapure water (1/10 v/v) and measured at 25°C with a dynamic light scattering angle of 90°C. The zeta potential was determined as follows: 200 μL (33.3 mg polymer/mL) of the samples was diluted in 2 mL of 0.1 mM KCl solution adjusted to pH 7.4. The average particle size was expressed as the volume mean diameter (Vmd) in nanometres (nm), and the average surface charge in milivolts (mV).

Shape and morphology were examined by scanning electron microscopy (SEM) in a ULTRA plus field emission scanning electron microscope (Carl Zeiss NTS GmbH, Oberkochen, Germany). For this purpose, freeze-dried formulations were placed in an eppendorf tube, resuspended in ultrapure water and centrifuged at 27 000 × g for 10 min at 4°C. Supernatants were discarded and the obtained pellets were again resuspended in ultrapure water. Then, 20 μL of suspension was mounted on carbon-coated transmission electron microscopy (TEM) sample grids (carbon film on 3 mm 400 mesh Cu grid, AGAR Scientific, Stansted, England) and placed in a desiccator in order to evaporate water. Finally, the grids were adhered with a double-sided adhesive tape onto metal stubs for SEM visualization.

The amount of the copolymer transformed into nanoparticles was determined by gravimetry from freeze-dried nanoparticles as described previously (Arbos et al., 2002). The yield was calculated from the difference between the initial amount of the copolymer used to prepare nanoparticles and the weight of the freeze-dried samples.

Chitosan analysis

The amount of chitosan associated to the particles was determined by UV–vis spectrophotometry. For this purpose, aliquots of the clear supernatants obtained during the purification steps were diluted with buffer solutions in accordance with the methodology developed by Muzzarelli (1998) and modified by Wischke and Borchert (2006). In brief, quantification of chitosan was performed using colorimetric determination due to the reaction of the dye with chitosan which results in a bathochromic shift. Cibacron Brilliant Red 3B-A (0.9 mg/mL) and 0.3 M glycine hydrochloride buffer (pH 3.2) were mixed with aliquots of the clear supernatants with unbounded chitosan. The method is sensitive and of a good reproducibility and linearity in the range 10–80 μg/mL. The absorbance values were measured at 575 nm, each sample was assayed in triplicate. The quantity of chitosan bound to the nanoparticles was calculated as the difference between the initial amount of chitosan added and the quantity of chitosan quantified in the supernatants and, thus, the chitosan loading was expressed as the amount of chitosan (in micrograms) per mg nanoparticles.

In vitro *release of RBITC from nanoparticles*

The amounts of RBITC loaded to nanoparticles were determined by colorimetry at wavelength 540 nm, respectively

(Labsystems iEMS Reader MF, Helsinki, Finland). The marker loading was calculated after total hydrolysis of a certain amount of nanoparticles in 0.1 M NaOH and expressed in μg/mg nanoparticles.

In vitro release of RBITC was studied by dispersion of nanoparticles (10 mg/mL) in both simulated gastric and intestinal fluids (USP XXXII) at 37°C. At predetermined time intervals, the nanosuspensions were centrifuged (34 000 × g, 15 min) and the RBITC released was quantified by measuring the supernatants by spectrofluorimetry (Perkin-Elmer, Waltham, MA, USA) at λ_{ex} 554 nm and λ_{em} 575 nm.

Bioadhesion studies

The bioadhesion study was performed using a protocol previously described (Arbós et al., 2003) in compliance with the regulations of the responsible Committee of the University of Navarra in line with the European legislation on animal experiments (86/609/EU). RBITC-loaded nanoparticles were administered orally to male Wistar rats fasted overnight (average weight 180 g, Harlan, Spain). The animals were divided in groups of three animals each ($n = 3$) and placed in metabolic cages and fasted overnight to prevent coprophagia but were allowed free access to water. The animals were housed under normal conditions and 12 h before the experiment were placed in metabolic cages and fasted overnight but with free access to water.

Each animal received a single oral dose of 1 mL aqueous suspension containing 10 mg of nanoparticles loaded with RBITC (45 mg particles/kg body weight). The nanoparticle suspension was given orally (intragastrically) to rats in a single administration using a long blunt animal feeding needle.

The animals were sacrificed by cervical dislocation at 1 h post-administration. The abdominal cavity was opened and the stomach, small intestine and caecum were removed. Then, the gut was divided into three anatomical regions: stomach (Sto), intestine and caecum (Ce). Each segment was opened lengthwise along the mesentery and rinsed with phosphate-buffered saline (PBS; pH 7.4).

Then, each washed segment (stomach, small intestine and caecum) was cut into four equal parts and digested in 1 mL of 3 M NaOH for 24 h. Afterwards, RBITC was dissolved in the digested samples by addition of 2 mL methanol, vortexed for 1 min and centrifuged at 6000 × g for 10 min. Aliquots (1 mL) of the resulting supernatants were assayed for RBITC by spectrofluorimetry at λ_{ex} 540 nm and λ_{em} 580 nm (GENios, TECAN, Grödig, Austria) in order to calculate the fraction of adhered nanoparticles to the mucosa. For calculations, standard curves of RBITC were prepared by addition of RBITC solutions (without nanoparticles) in 3 M NaOH (0.5–10 μg/mL) to control tissue segments following the same treatment steps of extraction ($r > 0.996$).

Tissue fluorescence microscopy studies

The tissue distribution of RBITC-loaded nanoparticles in the gastrointestinal mucosa was visualized by fluorescence microscopy (Olympus CH40 Model, Olympus, Barcelona, Spain). For that purpose, 10 mg of RBITC-labelled nanoparticles was orally administered to rats as described above. The animals were sacrificed 1 h later and the ileum was removed and washed with PBS. Then, mucosal portions from the ileum of about 0.5 cm length were treated with the tissue proceeding medium O.C.T., immersed in melting isopentane and frozen in liquid nitrogen. Tissue samples were cut into 5 μm sections in a cryostat (2800 Frigocut E, Germany), attached to poly-L-lysine precoated slides (Sigma, Madrid, Spain) and stored at −20°C before fluorescence microscopy visualization.

Statistical analysis

Data are expressed as the mean ± SD of at least three experiments. The Student's *t*-test assessed the nanoparticle characterization. For bioadhesion study, the analysis was processed using the non-parametric Kruskal–Wallis test, followed by Mann–Whitney *U*-test. Statistically significant differences were considered for *p*-values of < 0.05. All calculations were performed using a statistical software program (SPSS® 6.1.2, Microsoft).

Results

Determination of the thiol group content

For this study, two different molecular weights chitosan (20 and 50 kDa) were used. Table 1 shows both the amount of total (disulphide bonds) and reduced thiols (free groups) of the different thioglycolic acid-chitosan derivatives (CH20–TGA, CH20–TGB, CH50–TGA and CH50–TGB) employed in this study.

Characterization of chitosan–poly(anhydride) nanoparticles

The main physico-chemical characteristics of chitosan–poly(anhydride) nanoparticles are summarized in Table 2. Generally, coating of poly(anhydride) nanoparticles with chitosan significantly increases the size of the nanoparticles compared to uncoated ones (about 300 nm *vs* 190 nm). On the contrary, the zeta potential of chitosan-coated poly(anhydride) nanoparticles was found to be significantly lower than that of conventional nanoparticles. By SEM (Figure 1), conventional nanoparticles were found to be spherical with a smooth surface and size close to that quantified by PCS. However, chitosan-coated nanoparticles displayed a completely different surface with irregularities and the presence of like-aggregates at the surface of nanoparticles as observed for CH20–TGA NP and CH50–TGB NP (Figure 1(b) and (c)).

Table 2. Physico-chemical characteristics of fluorescently labelled chitosan-coated poly(anhydride) nanoparticles.

	Size (nm)	PDI	Zeta potential (mV)	Chitosan content (μg/mg)	RBITC content (μg/mg)
NP	191 ± 4	0.12	−51.1 ± 0.1		
CH20 NP	312 ± 6*	0.06	−32.3 ± 0.5*	4.65 ± 0.04	8.5 ± 0.1
CH20–TGA NP	304 ± 5*	0.05	−30.4 ± 0.5*	4.67 ± 0.26	8.8 ± 0.2
CH20–TGB NP	299 ± 12*	0.16	−32.7 ± 0.8*	4.74 ± 0.20	8.8 ± 0.2
CH50 NP	296 ± 3*	0.11	−30.3 ± 0.1*	4.67 ± 0.20	8.8 ± 0.1
CH50–TGA NP	313 ± 6*	0.14	−30.3 ± 0.2*	4.60 ± 0.25	8.7 ± 0.3
CH0–TGB NP	234 ± 5*	0.11	−32.9 ± 0.2*	477 ± 0.16	8.5 ± 0.2

Notes: Date are expressed as the mean ± SD ($n = 6$).
PDI, polydispersity index.
NP, poly(anhydride) nanoparticles; CH20 NP or CH50 NP, nanoparticles coated with unmodified chitosan; CH20–TGA NP or CH50–TGA NP, nanoparticles coated with low-thiol content chitosan; and CH20–TGB NP or CH50–TGB NP, nanoparticles coated with high-thiol content chitosan.
*$p < 0.05$; chitosan-coated nanoparticles *versus* control nanoparticles (NP) (Student's *t*-test).

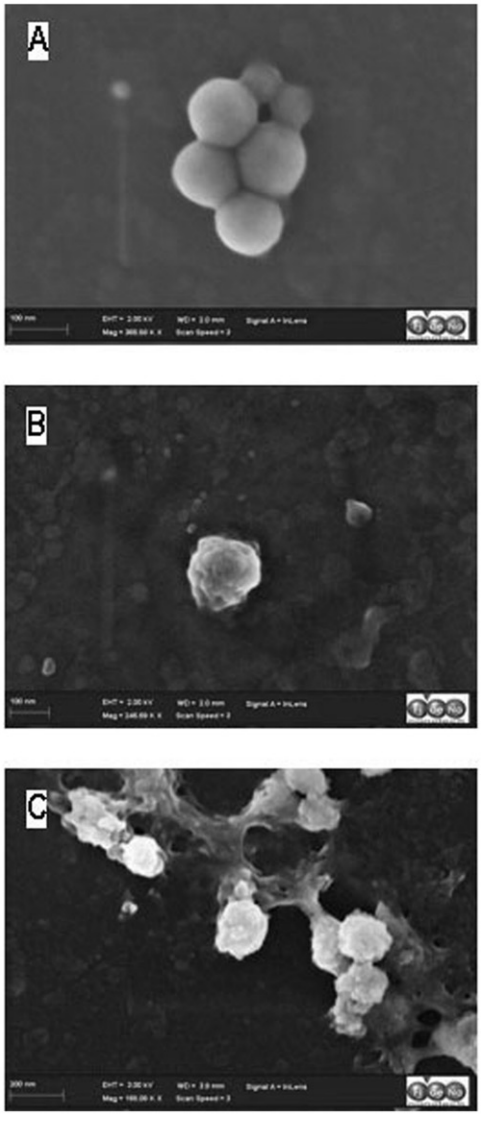

Figure 1. SEM microphotographs from: (a) chitosan–poly(anhydride) nanoparticles NP, (b) CH20–TGA NP and (c) CH50–TGA NP.

On the other hand, the yield of the process was calculated to be about 90%. Interestingly, the amount of polysaccharide associated to the nanoparticles was found to be similar for all the types of chitosans used (about 4.7 μg/mg) which corresponded to a binding efficiency of about 93%. Finally, the amount of RBITC incorporated in nanoparticles was about 8.5 μg/mg nanoparticles.

In vitro *release of RBITC from nanoparticles*

To ensure that the fluorescence determined in the gastrointestinal segments was due to the RBITC-associated nanoparticles, *in vitro* release of RBITC was preliminarily examined. Since the cumulative amount of RBITC released (30 min post-incubation in gastric fluid and other 60 min post-incubation in intestinal simulated fluids) was under the quantification limit of the analytical technique, it could be assumed that the measured fluorescence would be due to the RBITC-associated nanoparticles.

Bioadhesion of nanoparticles in the gastrointestinal tract

Figure 2 shows the adhered amount of nanoparticles (expressed in percentage) to the whole gastrointestinal tract over time (60 min) for the different formulations tested. Interestingly, the percentage of the adhered dose for nanoparticles coated with 20 kDa chitosan displayed a higher ability to develop adhesive interactions within the gut compared to that when coated with 50 kDa chitosan. This phenomenon was independent of thiolation. In fact, for all the nanoparticles coated with the low-molecular weight chitosan, the adhered fraction was around 30–35% of the given dose. On the other hand, when the nanoparticles were coated with high-molecular weight chitosan, they appear to have no effect on the bioadhesion since the adhesive capacity of NP (control nanoparticles) was similar to that observed for nanoparticles coated with CH50, CH50–TGA or CH50–TGB ($p > 0.05$).

Tissue fluorescence

Figure 3 shows fluorescence microscopy images of ileum samples from the animals treated with 10 mg of nanoparticle formulations, characterized by red fluorescent spots

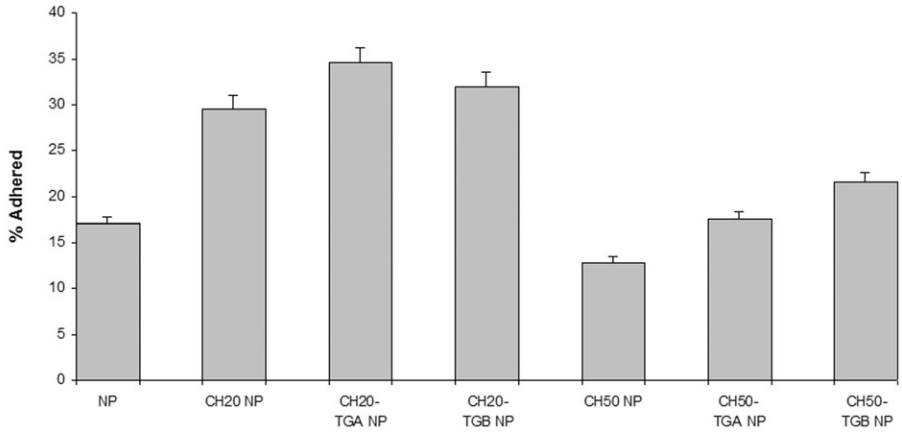

Figure 2. The total adhered amount of the nanoparticle formulations expressed in percentage. NP (poly(anhydride) nanoparticles); CH20 NP or CH50 NP, nanoparticles coated with unmodified chitosan; CH20–TGA NP or CH50–TGA NP, nanoparticles coated with low-thiol content chitosan; and CH20–TGB NP or CH50–TGB NP, nanoparticles coated with high-thiol content chitosan.

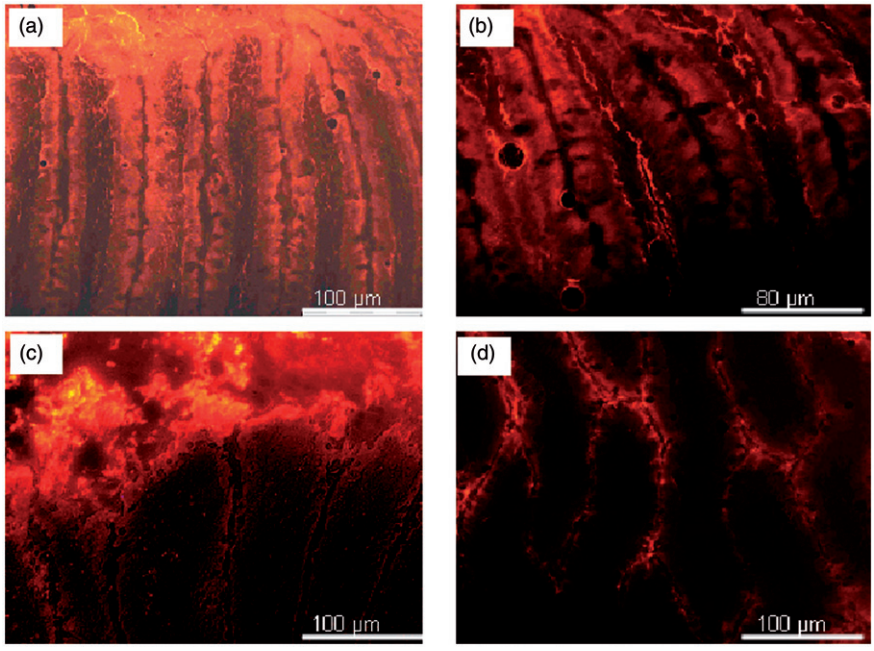

Figure 3. Fluorescence microscopy images of ileum samples. (a, b) CH20 NP, (c) CH50 NP, and (d) conventional nanoparticles.

(due to RBITC). CH20–TGA NP was found broadly distributed in terms of their adhesion to the ileum mucosa showing the high penetration capacity in the tissue layers (Figure 3(a) and (b)). On the contrary, CH50–TGA NP (Figure 3(c)) displayed a restricted localization in the mucosa, mainly in the outer layer of the ileum (mucus layer), which was similar to conventional nanoparticles (Figure 3(c)).

Discussion

In the past years, poly(anhydride) (Gantrez AN) nanoparticles have demonstrated a high ability to develop bioadhesive interactions within the gastrointestinal tract (Arbós et al., 2003). Their surface can be easily modified by simple incubation with different molecules or ligands in order to modify their distribution within the gut or/and their bioadhesive potential (Arbós et al., 2003; Salman et al., 2005; Yoncheva et al., 2005; Salman et al., 2006; Agüeros et al., 2009; Porfire et al., 2010). Thus, in this study, the idea was to modify these nanoparticles by their coating with biopolymers well known by their bioadhesive potential, such as chitosan. Chitosan has been proposed as adhesive material to increase the residence time of pharmaceutical dosage forms in close contact with the mucosa (Bernkop-Schnürch et al., 2003). In addition, chitosan would enhance the permeability of drugs through the opening of tight junctions between epithelial cells (Fernandez-Urrusuno et al., 1999).

More recently, many modifications of chitosan have been done in order to improve its potential characteristics in drug delivery (Shantha and Harding, 2002). In this context, chitosan was chemically modified by introduction of sulphhydryl groups yielding a new generation of bioadhesive polymers bearing thiol groups on their

backbone, the so-called thiomers (Bernkop-Schnürch et al., 1999, 2004; Leitner et al., 2003; Bernkop-Schnürch 2005; Elhassan and Bernkop-Schnürch, 2005; Föger et al., 2006).

Poly(anhydride) nanoparticles were successfully coated with chitosan, independent of both molecular weight and the degree of thiolation. For this purpose, the freshly prepared nanoparticles were incubated in an aqueous medium with the selected chitosan for 1 h at room temperature. During the optimization of the coating process, the optimal chitosan/poly(anhydride) ratio was fixed to be 0.5. In fact, higher ratios induce the formation of large aggregates (data not shown).

The coating of nanoparticles with chitosan induced both an increase of the size (about 100 nm) and a significant decrease of the negative zeta potential of the resulting nanoparticles. This last result appears to be in contradiction with previous results in which unmodified chitosan nanoparticles display net positive zeta potentials (Maculotti et al., 2005; Lee et al., 2006). Nevertheless, our results agree well with the fact that anhydride residues are highly reactive with amine primary groups (Ladaviere et al., 2000) and this phenomenon has been previously used by Cerchiara et al. (2005) to prepare microparticles from chitosan and the copolymer between methyl ether and maleic anhydride for nasal delivery.

Thus, the interaction between the primary amino groups of chitosan and the anhydride residues of the polymer would consume the ionizable amino groups and, therefore, the possibility for the resulting nanoparticles to develop positive charges. This hypothesis would also be supported by the fact that all the nanoparticle formulations displayed similar chitosan content (about 4.7 μg/mg nanoparticle), which can be a direct proof of a saturation phenomenon.

On the other hand, when poly(anhydride) nanoparticles were coated with chitosan, they displayed a different bioadhesive capacity which appeared to be dependent on the MW of the polysaccharide employed. Thus, nanoparticles coated with 20 kDa chitosan (CH20–TG NP) showed an adhesive capacity about two times higher than NP. On the contrary, NP showed a bioadhesive capacity about 1.3 times higher than nanoparticles coated with 50 kDa chitosan. This observation agrees with the published work by Bravo-Osuna et al. (2006), in which they observed a higher adhesion tendency of poly(alkylcyanoacrylate) nanoparticles coated with 20 kDa chitosan than with 50 kDa chitosan. Other authors had already pointed out the existence of a direct relationship between the molecular weight of chitosans and their bioadhesive capacity (Felt et al., 1999; Takeuchi et al., 2005). This may be due to the interpenetration mechanisms with the mucus chains. In fact, the extent of interpenetration, which is essential for high bioadhesive properties (Imam et al., 2003), is strongly reduced when the polymer chains are too long.

Figure 3 shows nanoparticle adhesion in rat non-follicular mucosa (normal enterocytes). These images confirm the ability of CH20 NP to diffuse through the mucus layer whereas those carriers coated with CH50 NP would remain adhered to the mucus layer. This observation may be due to the inverse correlation between the molecular weight of the chitosan used to coat poly(anhydride) nanoparticles and, thus, by the higher length of the polymer chains than for chitosan 20 and the bioadhesive capacity.

When nanoparticles were coated with thiolated chitosan, they displayed slightly higher ability to develop bioadhesive interactions than nanoparticles decorated with unmodified chitosan. These results are in agreement with previous observations concerning the increasing potential of chitosan carriers as mucosal drug delivery systems when the polysaccharide had been previously thiolated. In this context, increments ranging between two- and fivefold in the intestinal bioadhesion have been reported for trimethyl chitosan nanoparticles (Lichen et al., 2009) and chitosan microparticles (Maculotti et al., 2005) or nanoparticles (Bravo-Osuna et al., 2007). In our case, the highest influence was observed with 50 kDa chitosan. Thus, nanoparticles coated with thiolated chitosan displayed between 1.3 (low thiol content) and 1.6 times (high thiol content) higher adhesive capacity than nanoparticles coated with unmodified chitosan.

In any case, this improvement in the ability of nanoparticles to develop adhesive interactions when coated with thiolated chitosans would be promoted by the formation of a cross-linked structure in the shell by creation of intra- and inter-chain disulphide bonds (Bravo-Osuna et al., 2008). In addition, this fact would improve the nanoparticle adhesion on intestinal tissues due to the development of non-covalent interactions (hydrogen bonds) between chemical groups of chitosan and several groups of mucus chains and covalent bonds between thiol groups of the nanoparticle surface and cysteine residues of the mucus glycoproteins (Richert et al., 2004; Bravo-Osuna et al., 2008).

Conclusions

This study has demonstrated the possibility of obtaining bioadhesive nanoparticles coated with either chitosans or their thiolated conjugates by a simple incubation method. The coating of nanoparticles with low-MW chitosan (CH20) increased the adhesive capacity of the nanoparticles. Finally, the coating of poly(anhydride) nanoparticles with thiolated chitosan improved their adhesive abilities. Thus, poly(anhydride) nanoparticles coated with thiolated chitosan can be considered as promising bioadhesive particulate carriers for oral delivery strategies.

Acknowledgements

The authors thank the staff of FideNA – PrincipiaTech – Navarra for their collaboration in SEM studies. J.M. Llabot thanks Consejo Nacional de Investigaciones

Científicas y Técnicas (CONICET) for a research fellowship. In addition, this research was supported by grants from the Department of Health of the Government of Navarra (Res. 2118/2007) and Foundation ''Caja Navarra'' (Project 10828: Nanotechnology and medicines) in Spain.

Declaration of interest

The authors report no declarations of interest.

References

Agüeros M, Campanero MA, Salman H, Quincoces G, Peñuelas I, Irache JM. Bioadhesive properties and biodistribution of cyclodextrin-poly(anhydride) nanoparticles. Eur J Pharm Sci, 2009;37 (3–4):231–40.

Ambruosi A, Yamamoto H, Kreuter J. Body distribution of polysorbate-80 and doxorubicin-loaded [14C]poly(butyl cyanoacrylate) nanoparticles after i.v. administration in rats. J Drug Target, 2005;13 (10):535–42.

Arbós P, Campanero MA, Arangoa MA, Renedo MJ, Irache JM. Influence of the surface characteristics of PVM/MA nanoparticles on their bioadhesive properties. J Control Release, 2003;89 (1):19–30.

Arbos P, Wirth M, Arangoa MA, Gabor F, Irache JM. Gantrez AN as a new polymer for the preparation of ligand-nanoparticle conjugates. J Control Release, 2002;83 (3):321–30.

Aumelas A, Serrero A, Durand A, Dellacherie E, Leonard M. Nanoparticles of hydrophobically modified dextrans as potential drug carrier systems. Colloids Surf B, 2007;59 (1):74–80.

Bernkop-Schnürch A. Thiomers: A new generation of mucoadhesive polymers. Adv Drug Deliv Rev, 2005;57 (11):1569–82.

Bernkop-Schnürch A, Hornof M, Guggi D. Thiolated chitosans. Eur J Pharm Biopharm, 2004;57 (1):9–17.

Bernkop-Schnürch A, Hornof M, Zoidl T. Thiolated polymers-thiomers: Synthesis and *in vitro* evaluation of chitosan-2-iminothiolane conjugates. Int J Pharm, 2003;260 (2):229–37.

Bernkop-Schnürch A, Schwarz V, Steininger S. Polymers with thiol groups: A new generation of mucoadhesive polymers? Pharm Res, 1999;16 (6):876–81.

Bravo-Osuna I, Schmitz T, Bernkop-Schnürch A. Elaboration and characterization of thiolated chitosan coated acrylic nanoparticles. Int J Pharm, 2006;316 (1–2):170–5.

Bravo-Osuna I, Vauthier C, Farabollini A, Millotti G, Ponchel G. Effect of chitosan and thiolated chitosan coating on the inhibition behaviour of PIBCA nanoparticles against intestinal metallopeptidases. J Nanopart Res, 2008;10 (8):1293–301.

Bravo-Osuna I, Vauthier C, Farabollini A, Palmieri GF, Ponchel G. Mucoadhesion mechanism of chitosan and thiolated chitosan-poly(isobutyl cyanoacrylate) core-shell nanoparticles. Biomaterials, 2007;28 (13):2233–43.

Cerchiara T, Luppi B, Chidichimo G, Bigucci F, Zecchi V. Chitosan and poly(methyl vinyl ether-co-maleic anhydride) microparticles as nasal sustained delivery systems. Eur J Pharm Biopharm, 2005;61 (3):195–200.

Choi SW, Kim JH. Design of surface-modified poly(D,L-lactide-co-glycolide) nanoparticles for targeted drug delivery to bone. J Control Release, 2007;122 (1):24–30.

Cui Z, Mumper RJ. Chitosan-based nanoparticles for topical genetic immunization. J Control Release, 2001;75 (3):409–19.

Damge C, Michel C, Aprahamian M, Couvreur P. New approach for oral administration of insulin with polyalkylcyanoacrylate nanocapsules as drug carrier. Diabetes, 1988;37 (2):246–51.

Damge C, Vranckx H, Balschmidt P, Couvreur P. Poly(alkyl cyanoacrylate) nanospheres for oral administration of insulin. J Pharm Sci, 1997;86 (12):1403–9.

Elhassan IM, Bernkop-Schnürch A. Controlled drug delivery systems based on thiolated chitosan microspheres. Drug Dev Ind Pharm, 2005;31 (6):557–65.

Esmaeili F, Ghahremani MH, Esmaeili B, Khoshayand MR, Atyabi F, Dinarvand R. PLGA nanoparticles of different surface properties: Preparation and evaluation of their body distribution. Int J Pharm, 2008;349 (1–2):249–55.

Felt O, Furrer P, Mayer JM, Plazonnet B, Buri P, Gurny R. Topical use of chitosan in ophthalmology: Tolerance, assessment and evaluation of precorneal retention. Int J Pharm, 1999;180 (2):185–93.

Fernandez-Urrusuno R, Romani D, Calvo P, Vila-Jato JL, Alonso MJ. Development of a freeze-dried formulation of insulin-loaded chitosan nanoparticles intended for nasal administration. STP Pharma Sci, 1999;9:429–36.

Florence AT. The oral absorption of micro- and nanoparticulates: Neither exceptional nor unusual. Pharm Res, 1997;14 (3):259–66.

Föger F, Schmitz T, Bernkop-Schnürch A. *In vivo* evaluation of an oral delivery system for P-gp substrates based on thiolated choosing. Biomaterials, 2006;27:4250–5.

Hassan EE, Gallo JM. A simple rheological method for the *in vitro* assessment of mucin-polymer bioadhesive bond strength. Pharm Res, 1990;7 (5):491–5.

Huang M, Wu W, Qian J, Wan DJ, Wei XL, Zhu JH. Body distribution and in situ evading of phagocytic uptake by macrophages of long-circulating poly (ethylene glycol) cyanoacrylate-co-n-hexadecyl cyanoacrylate nanoparticles. Acta Pharmacol Sin, 2005;26:1512–18.

Imam ME, Hornof M, Valenta C, Reznicek G, Bernkop-Schnürch A. Evidence for the interpenetration of mucoadhesive polymers into the mucus gel layer. STP Pharma Sci, 2003;13 (3):171–6.

Kast CE, Bernkop-Schnürch A. Thiolated polymers – thiomers: Development and *in vitro* evaluation of chitosan-thioglycolic acid conjugates. Biomaterials, 2001;22 (17):2345–52.

Ladaviere C, Lorenzo C, Elaissari A, Mandrand B, Delair T. Electrostatically driven immobilization of peptides onto (maleic anhydride-alt-methyl vinyl ether) copolymers in aqueous media. Bioconjugate Chem, 2000;11 (2):146–52.

Lee DW, Shirley SA, Lockey RF, Mohapatra SS. Thiolated chitosan nanoparticles enhance anti-inflammatory effects of intranasally delivered theophylline. Respir Res, 2006;7 (1):112.

Leitner VM, Walker GF, Bernkop-Schnürch A. Thiolated polymers: Evidence for the formation of disulphide bonds with mucus glycoproteins. Eur J Pharm Biopharm, 2003;56 (2):207–14.

Lichen Y, Jieying D, Chunbai H, Liming C, Chunhua Y. Drug permeability and mucoadhesion properties of thiolated trimethyl chitosan nanoparticles in oral insulin delivery. Biomaterials, 2009;30 (29):5691–700.

Maculotti K, Genta I, Perugini P, Imama M, Bernkop-Schnürch A, Pavanetto F. Preparation and *in vitro* evaluation of thiolated chitosan nanoparticles. J Microencapsulation, 2005;22 (5):459–70.

Muzzarelli RA. Colorimetric determination of chitosan. Anal Biochem, 1998;260 (2):255–7.

Pandey R, Ahmad Z, Sharma S, Khuller GK. Nano-encapsulation of azole antifungals: Potential applications to improve oral drug delivery. Int J Pharm, 2005;301 (1–2):268–76.

Perera G, Greindl M, Palmberger TF, Bernkop-Schnürch A. Insulin-loaded poly(acrylic acid)-cysteine nanoparticles: Stability studies towards digestive enzymes of the intestine. Drug Deliv, 2009;16 (5):254–60.

Ponchel G, Irache J. Specific and non-specific bioadhesive particulate systems for oral delivery to the gastrointestinal tract. Adv Drug Deliv Rev, 1998;34 (2–3):191–219.

Porfire AS, Zabaleta V, Gamazo C, Leucuta SE, Irache JM. Influence of dextran on the bioadhesive properties of poly(anhydride) nanoparticles. Int J Pharm, 2010;390 (1):37–44.

Richert L, Lavalle P, Payan E, Shu XZ, Prestwich GD, Stoltz JF, Schaaf P, Voegel JC, Picart C. Layer by layer buildup of polysaccharide films: Physical chemistry and cellular adhesion aspects. Langmuir, 2004;20 (2):448–58.

Sahana DK, Mittal G, Bhardwaj V, Kumar MN. PLGA nanoparticles for oral delivery of hydrophobic drugs: Influence of organic solvent on nanoparticle formation and release behavior *in vitro* and *in vivo* using estradiol as a model drug. J Pharm Sci, 2008;97 (4):1530–42.

Salman HH, Gamazo C, Campanero MA, Irache JM. Salmonella-like bioadhesive nanoparticles. J Control Release, 2005;106 (1–2):1–13.

Salman HH, Gamazo C, Campanero MA, Irache JM. Bioadhesive mannosylated nanoparticles for oral drug delivery. J Nanosci Nanotechnol, 2006;6 (9–10):3203–9.

Shantha KL, Harding ORK. Synthesis and characterization of chemically modified chitosan microspheres. Carbohydr Polym, 2002;48 (3):247–53.

Soares AF, Carvalho A, Veiga F. Oral administration of peptides and proteins: Nanoparticles and cyclodextrins as biocompatible delivery systems. Nanomedicine, 2007;2 (2):183–202.

Takeuchi H, Thongborisute J, Matsui Y, Sugihara H, Yamamoto H, Kawashima Y. Novel mucoadhesion tests for polymers and

polymer-coated particles to design optimal mucoadhesive drug delivery systems. Adv Drug Del Rev, 2005;57 (11):1583–94.

Thanou M, Verhoef JC, Junginger HE. Oral drug absorption enhancement by chitosan and its derivatives. Adv Drug Deliv Rev, 2001;52 (2):117–26.

Van der Merwe SM, Verhoef JC, Kotze AF, Junginger HE. N-trimethyl chitosan chloride as absorption enhancer in oral peptide drug delivery. Development and characterization of minitablet and granule formulations. Eur J Pharm Biopharm, 2004;57 (1):85–91.

Wischke C, Borchert HH. Increased sensitivity of chitosan determination by a dye binding method. Carbohydr Res, 2006;341 (18):2978–9.

Yoncheva K, Lizarraga E, Irache JM. Pegylated nanoparticles based on poly(methyl vinyl ether-co-maleic anhydride): Preparation and evaluation of their bioadhesive properties. Eur J Pharm Sci, 2005;24 (5):411–19.